VERTEBRATE BIOLOGY

REVISTA DE Biología Tropical

https://doi.org/10.15517/hbbz6m79

Morphometry and histochemistry of the gastrointestinal tract of *Curimata mivartii* (Characidae: Curimatidae)

Diana Sofía Luna-Gómez[1]; https://orcid.org/0009-0007-5053-8270
Roger Iván Valderrama-Londoño[1]; https://orcid.org/0009-0003-3946-3766
Luisa F. Londoño-Ramírez[1]; https://orcid.org/0000-0002-5387-0689
Ana Estrada-Posada[2]; https://orcid.org/0000-0003-3585-3719
Jonny Andrés Yepes-Blandón*[1]; https://orcid.org/0000-0001-6276-5488

1. Grupo de Investigación en Organismos Acuáticos Nativos y Exóticos (GIOANE), Instituto de Biología, Universidad de Antioquia, Medellín, Colombia. diana.lunag@udea.edu.co; roger.valderrama@udea.edu.co; luisa.londonor@udea.edu.co; jonny.yepes@udea.edu.co (*Correspondencia)
2. ISAGEN S.A. E.S.P, Medellín, Antioquia, Colombia; aestrada@isagen.com.co

Received 04-VII-2025. Corrected 07-I-2026. Accepted 18-III-2026.

ABSTRACT

Introduction: *Curimata mivartii* is a freshwater fish endemic to the Magdalena-Cauca Basin in Colombia and classified as vulnerable to extinction due to habitat fragmentation, overfishing, climate change, and pollution. Understanding the gastrointestinal tract (GIT) characteristics is essential for developing appropriate nutrition protocols for captive breeding and conservation efforts.

Objectives: To characterize the morphological, histological, and histochemical features of the gastrointestinal tract of adult *C. mivartii* specimens and identify adaptations related to their detritivorous feeding habits**.**

Methods: In March 2022, 22 adult specimens (average weight: 177.5 ± 27.9 g) were analyzed using morphometric measurements, histological techniques, histochemical staining for mucin identification, and transmission electron microscopy (TEM) to examine the ultrastructure of the GIT.

Results: The GIT consists of a short esophagus with abundant mucus-producing goblet cells and rare acinar glands, a curved stomach with distinct cardiac, fundic, and pyloric regions, and densely coiled pyloric caeca intestine. The pyloric stomach is protected by a thick koilin membrane, like the gizzard in birds, indicating adaptation to a high-fiber detritus diet. Neutral mucins were detected throughout GIT, while carboxylated acidic mucins predominated in the intestine, suggesting specialized interactions with beneficial microbiota. TEM revealed specialized cellular adaptations in each GIT region, including microridges on esophageal epithelial cells, microvilli of gastric columnar cells, and the brush border of enterocytes.

Conclusions: The GIT features of *C. mivartii* reflect adaptations to detritus assimilation and microphagy, with the comprehensive mucin mapping providing valuable insights for optimizing captive breeding protocols. These findings establish a foundation for future research on pathologies, diet adaptability, and nutritional health status of this vulnerable native species.

Key words: detritivorous fish; digestive morphology; koilin membrane; microbiota, interactions; conservation breeding.

RESUMEN

Morfometría e histoquímica del tracto gastrointestinal de *Curimata mivartii* (Characidae: Curimatidae)

Introducción: *Curimata mivartii* es un pez de agua dulce endémico de la cuenca Magdalena-Cauca en Colombia y clasificado como vulnerable a la extinción debido a la fragmentación del hábitat, la sobrepesca, el cambio climático y la contaminación. Comprender las características del tracto gastrointestinal (TGI) es fundamental para desarrollar protocolos de alimentación adecuados para la cría en cautiverio y en los esfuerzos de conservación.
Objetivos: Caracterizar la morfología, histología e histoquímica del tracto gastrointestinal de adultos de *C. mivartii* e identificar adaptaciones relacionadas con sus hábitos alimentarios detritívoros.
Métodos: En marzo de 2022, se analizaron 22 especímenes adultos (peso promedio 177.5 ± 27.9 g) mediante mediciones morfométricas, técnicas histológicas, tinciones histoquímicas para la identificación de mucinas y microscopía electrónica de transmisión (TEM) para examinar la ultraestructura del TGI.
Resultados: El TGI consta de un esófago corto con abundantes células caliciformes productoras de moco y glándulas acinares únicas, un estómago curvo con regiones cardíaca, fúndica y pilórica bien definidas, ciegos pilóricos y un intestino densamente enrollado. El estómago pilórico está protegido por una gruesa membrana de koilina similar a la molleja de las aves, lo que indica una adaptación a una dieta rica en detritos fibrosos. Se detectaron mucinas neutras a lo largo de todo el TGI, mientras que las mucinas ácidas carboxiladas predominaron en el intestino, lo que sugiere interacciones especializadas con microbiota benéfica. La TEM reveló adaptaciones celulares especializadas en cada región del TGI, incluyendo microcrestas en las células epiteliales esofágicas, microvellosidades en las células columnales gástricas y el borde en cepillo de los enterocitos.
Conclusiones: Las características del TGI de *C. mivartii* reflejan adaptaciones para la asimilación de detritos y la microfagia, y el mapeo detallado de mucinas proporciona información valiosa para optimizar los protocolos de cría en cautiverio. Estos hallazgos establecen una base para futuras investigaciones sobre patologías, adaptabilidad dietaria y estado nutricional de esta especie nativa vulnerable.

Palabras clave: peces detritívoros; morfología digestiva; membrana koilin; microbiota; interacciones; cría de conservación.

INTRODUCTION

The vizcaina, *Curimata mivartii* (Steindachner, 1878), (Characiformes, Curimatidae), is a fish species endemic to the Magdalena-Cauca Basin in Colombia and the sole representative of the genus *Curimata* in the trans-Andean region (Vari, 1989b). Habitat fragmentation, destruction, overfishing, climate change, and pollution within the Magdalena Basin have contributed to the species being classified as vulnerable on both Colombia's Red List of Freshwater Species (Mojica et al., 2012) and the International Union for Conservation of Nature (IUCN) Red List of Threatened Species (Jiménez-Segura, 2016). The population size of *C. mivartii* is estimated to have declined by 30 %, with no improvement in its vulnerability status since 2002 (Sánchez-Duarte & Lasso, 2013). This decline and its environmental and ecological consequences directly impact riparian communities' economy and food security. *C. mivartii* is a detritivorous species that feeds by suctioning submerged roots in riverbanks and wetlands at depths of less than 4.5 m (Jiménez-Segura & Lasso, 2020; Lasso et al., 2011).

The species performs short reproductive migrations (≈ 11 km) from tributary rivers to the main channel (López-Casas et al., 2016). Its eggs and larvae complete their developmental stages in downstream wetlands and riverbanks, where they grow until reaching sexual maturity and restarting the migratory cycle. The reproductive dynamics of the species are closely linked to the duration of the rainy and dry seasons, which regulate water levels in breeding areas, ensuring the entry and development of eggs and larvae. As a result, the species are particularly vulnerable to deforestation and climate change (Jiménez-Segura et al., 2010).

To date, published studies on this species include migration patterns (Jiménez-Segura et al., 2010; López-Casas et al., 2016), population genetics using microsatellites (Landínez-García

& Marquez, 2018), captive breeding with hormonal protocols (Montes-Petro et al., 2019), morphometry (Hincapié-Cruz & Márquez, 2021), and embryonic development (Giraldo-Sarmiento, 2022). Regarding the digestive system, some anatomical features of the oropharyngeal cavity in adult fish have been described. These serve as synapomorphies for diagnosing the family Curimatidae and the genus *Curimata* (Vari, 1989a; Vari, 1989b). One such feature is the presence of abundant buccal folds composed of soft and mucus-producing tissue, involved in forming the food bolus (Vari, 1989b). The developmental stages of the digestive tract through the larval and juvenile stages are also known (Giraldo-Sarmiento, 2022). However, no published studies exist on the anatomical and histochemical characteristics of the digestive system in adults of *C. mivartii*. This information is essential to complement previous studies and enhance understanding of the species' biology, thereby facilitating the development of appropriate nutrition protocols for captive breeding.

The fish's digestive system is divided into the buccopharyngeal cavity, esophagus, stomach, and the anterior, middle, and posterior intestines. These segments correspond, respectively, to the functions of capturing, chewing, and swallowing; digestion and nutrient absorption; and excretion. However, besides ontogenetic and phylogenetic variations, fish can exhibit adaptations and specializations in the organs and tissues of the gastrointestinal tract (GIT) that enhance nutrient utilization based on their diet. One example of this is the biological diversity found in fish of the order Characiformes, where the adaptability of the digestive system to optimize food capture, ingestion, digestion, and absorption has allowed them to colonize a wide range of ecological niches in the Neotropics (Lavoué et al., 2017).

Adaptations in the digestive system can also occur at the histological level within the concentric layers that make up the digestive tract wall: the mucosal tunic, submucosal tunic, muscular tunic, and serosal tunic (Wilson & Castro, 2010). Among these layers, the mucosal tunic shows the greatest variability, as it is in direct contact with both the environment and food. The tissue's interaction with the environment is mediated by gastrointestinal mucus produced by goblet cells in the mucosal tunic. This mucus serves several functions, including lubrication to facilitate food movement, protection against mechanical damage, defense against pathogens, nutrient absorption, and other non-digestive functions, such as osmoregulation and respiration (Salinas & Parra, 2015).

Gastrointestinal mucus is composed of 95 % water and 5 % proteins known as mucins. Mucins are glycosylated proteins with long polysaccharide side chains, which account for more than 70 % of their molecular weight. The spatial distribution and ionic interactions of the sugar chains in mucins with the aqueous medium contribute to the mucus's viscosity, hydration, and protective properties (Allen, 1983). Based on the net ionic charge of the polysaccharide chains, mucins are classified as acidic or neutral. Neutral mucins contain uncharged sugars such as fucose and galactose, while acidic mucins are glycosylated with sialic acid residues (sialomucins) or ester sulfates (sulfomucins) (Allen, 1983; Gona, 1979). The composition of polysaccharides in mucins can vary depending on the tissue of origin, species, and regions of the gastrointestinal tract (Díaz et al., 2003; Mantle & Allen, 1981). Therefore, studying their distribution in the gastrointestinal tract of a species can provide valuable insights into the physiological and environmental adaptations of the tissues.

To identify mucin types, a combination of histochemical stains is used: periodic acid-Schiff (PAS) for neutral mucins and Alcian Blue (AB) for acidic mucins. In PAS staining, periodic acid breaks the glycosidic bonds of monosaccharides in the sugar chains, converting glycol groups into aldehyde groups, which then bind to the amino groups of the Schiff reagent. This technique is typically used to identify molecules with a high content of neutral sugars. AB staining, on the other hand, employs cationic dye, and an acidic environment is required to ionize the sugar residues

for effective binding to mucins. To identify acidic mucins with carboxyl and sulfate ester groups, a pH of 2.5 is used, while a more acidic pH of 1.0 is employed to identify sulfate esters specifically. By combining PAS and AB stains, both acidic and neutral mucins can be detected simultaneously in a tissue. In PAS/AB combined staining, goblet cells may stain pure blue, pure red, or a combination of both colors. With PAS/AB at pH 2.5, blue-stained cells produce predominantly acidic glycoproteins (sialomucins and sulfomucins), while red-stained cells produce neutral glycoproteins. At PAS/AB pH 1.0, neutral glycoproteins stain red, and acid-sulfated glycoproteins stain blue (Fletcher et al., 1976; Neuhaus et al., 2007).

Understanding the characteristics and adaptations of a species' digestive tract is essential for comprehending the mechanisms of nutrient absorption, digestion, and excretion and inferring its feeding habits. This knowledge provides valuable insights for formulating appropriate diets, managing feeding practices, planning polyculture systems, and identifying pathological and physiological alterations related to infections, environmental pollution, and artificial diets. It significantly contributes to conservation programs for native species and helps expand the limited information available on Neotropical ichthyofauna (Alonso et al., 2015; Burns, 2021; Da Silva, 2016; Guisande et al., 2012).

This study examined *C. mivartii*'s gastrointestinal tract's characteristics using morphometry, histology, mucin histochemistry, and transmission electron microscopy (TEM). The goal was to inform the development of feeding protocols for captive breeding.

MATERIALS AND METHODS

Ethics Statement: All procedures involving animal handling were conducted in accordance with the Guide for the Care and Use of Laboratory Animals (Albus, 2012), and in accordance with the Resolution 0955 of May 27, 2020, issued by the Colombian National Aquaculture and Fisheries Authority (Autoridad Nacional de Acuicultura y Pesca [AUNAP], 2020), which granted the research permit to Piscícola San Silvestre.

Study site: The research was conducted at Piscícola San Silvestre S.A. (PSS), located in the city of Barrancabermeja, Santander (7°06'31" N & 73°51'23" W), at an elevation of 75 m. a. s. l., with an average annual temperature of 28.4 °C and 75 % relative humidity. Fish were collected in March 2022 from the Sogamoso River, a tributary of the Magdalena River, where PSS captures species for breeding and relocation.

Fish sampling: The specimens were captured using a cast net. A total of 22 individuals were transported to the PSS in 800 L plastic tanks containing river water and continuously aerated with an air pump. Upon arrival at the PSS, specimens were immediately processed, and body weight (BW), total length (TL), and standard length (SL) were measured. One individual was randomly selected for anatomical description and photographic documentation, 15 were used for morphological parameter assessment, and six were allocated for histological and histochemical analyses. Photographic registry of the dissection and anatomical features was performed with an EOS Rebel T3i camera with a Canon EF-S 18-55 mm f/4-5.6 IS STM lens.

Morphological parameters and body indexes: Fifteen individuals were randomly selected, anesthetized with pharmaceutical-grade eugenol (10 ppm), and euthanized by severing the spinal cord between the posterior end of the skull and the dorsal fin. To dissect the digestive tract, a crescent-shaped incision was made from the dorsal edge of the operculum to the anal papilla, followed by a cut below the lateral line and a longitudinal incision extending toward the cranial region. The skin flap was removed to expose and extract the gastrointestinal tract (esophagus, stomach, and intestine), liver, gonads, and gills. The length (cm) and weight (g) of these organs were measured using an ichthyometer and a precision scale (Ohaus®).

Based on the measurements of body weight (BW), gonad weight (GW), liver weight (LW), eviscerated weight (EW), total length (TL), and intestinal length (IL), the following morphometric indexes were calculated:

- $Condition\ Factor\ (K) = \frac{BW}{TL^3}\ x100$
- $Instestinal\ Coefficient\ (I.C) = \frac{IL}{TL}$
- $Zihler's\ Index\ (ZI) = \frac{IL}{(10*\frac{BW}{3})}$
- $Gonadosomatic\ Index\ (GI) = \frac{GW}{BW}\ x100$
- $Hepatosomatic\ Index = \frac{LW}{TW}\ x100$

Histology and histochemistry: Extracted tissues of six randomly selected specimens were fixed in 10 % buffered formalin for 24 hours. To enhance preservation, formalin was also infused into the lumen of tubular organs. For histological slide preparation, the tissues were rinsed with 70 % alcohol and dehydrated using a graded series of alcohol solutions (30 %-100 %). The tissues were treated with toluene to remove residual alcohol and embedded in hot paraffin. Paraffin block molding and storage were performed at room temperature, and sections measuring 5-6 µm were cut from each block using a Leica rotary microtome. The sections were stained with hematoxylin and eosin (H&E) to describe histological layers and assess qualitative morphostructural features using an Olympus CX23 optical microscope and a Basler ACA54-17 digital camera.

Histochemistry: Histochemical staining was performed according to the protocol described by Vidal et al. (2020) for histological analysis of mucin distribution. The staining techniques included Masson'sTrichromic to differentiate connective and muscle tissues, PAS for detecting neutral mucins, AB at pH 2.5 for identifying carboxylated and sulfated acidic mucins, and AB at pH 1.0 for detecting exclusively sulfated acidic mucins. To examine the association of acidic and neutral mucins, AB staining at pH 2.5 was followed by PAS. Additionally, a mucicarmine kit was employed to visualize epithelial acidic mucins.

Transmission Electron Microscopy (TEM): To TEM images of the epithelial tissue from each intestinal region, tissue fragments were fixed in 2.5 % glutaraldehyde buffered in PBS, followed by post-fixation in 1 % osmium tetroxide and 3 % uranyl acetate. The fragments were subjected to a progressive dehydration process and infiltrated with plastic resin using a 1:1 acetone solution for embedding in SPURR resin (Electron Microscopy Sciences, Fort Washington, PA, USA). Resin blocks were sectioned with a Sorvall MT2-B ultramicrotome. Semi-thin sections (1 µm) were stained with toluidine blue to identify the most appropriate areas for ultra-thin sectioning. These regions were cut to a thickness of 80-100 nm (yellow-gold interference color) using a diamond knife and placed on 200 mesh copper grids. The sections were then contrasted with uranyl acetate and lead citrate and examined and photographed with a JEOL 1400 Plus transmission electron microscope at the Pathology Department of the Fundación Santa Fe de Bogotá University Hospital.

Data analysis: A completely randomized experimental design was applied, and descriptive statistics were used to characterize the sample regarding morphological parameters and body indexes. All parameters and indexes are presented as the mean ± standard deviation (SD). The histochemical results for mucins were interpreted based on the staining intensity of the tissue for each staining technique. The intensity level was determined through visual inspection, and the staining intensities were recorded using a +/- scale, as described by Diaz et al. (2008) and Vidal et al. (2020). The staining intensities were categorized as follows: (-) negative staining, (+) mild staining, (++) moderate staining, and (+++) strong staining.

RESULTS

Body indexes and morphological parameters: The sample of 15 specimens (6 males and 9 females) of *C. mivartii* (Fig. 1A) had an average weight of 177.5 ± 27.9 g, a TL of 23.2 ± 2.6 cm, and a SL of 18.1 ± 1.9 cm. The species does not show sexual dimorphism, and sex was

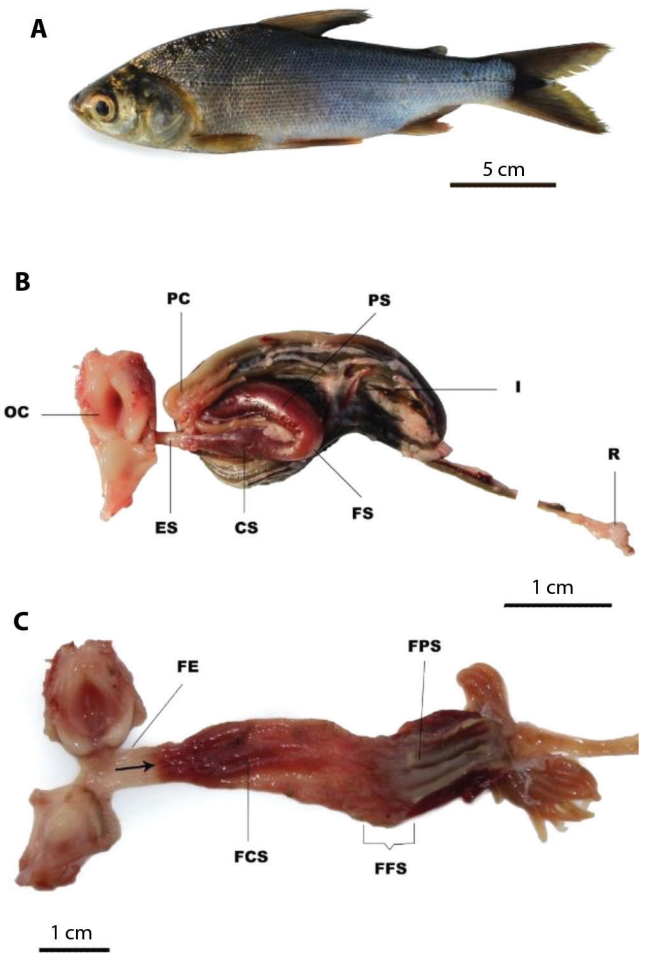

Fig. 1. A. Complete external morphology of adult *Curimata mivartii* (side view): cephalic region (head), abdominal region (visceral cavity), and caudal region (peduncle and caudal fin). **B.** Anatomy of the gastrointestinal tract located in the ventral coelomic cavity. It begins with the oropharyngeal cavity (OC), continues with the esophagus (ES) in the dorsocaudal region of the gills, and the curved stomach in the anterior abdominal region ventral to the swim bladder. The stomach includes the cardiac (CS), fundic (FS), and pyloric (PS) regions. The pyloric caeca (PC) are oriented toward the ventral and lateral abdominal cavity, around the beginning of the intestine. The intestine (I) is coiled in the middle and caudal abdominal region in several loops until it reaches the rectum (R), which ends in the caudal abdominal region. **C.** Folds of esophagus (FE), cardiac stomach (FCS), fundic stomach (FFS) and pyloric stomach (FPS), note the yellow superficial membrane like the cuticle found in avian ventriculus.

determined by the presence of female or male gonads during dissection (Table 1). No significant differences were observed between sexes for any of the biometric indices evaluated. The condition factor (K) for the sample was 0.96 ± 0.24, with one specimen falling below the average, having a value of 0.44. The gonadosomatic index (GSI) for females averaged 11.2 ± 4.7, while for males it was 0.8 ± 0.3. The hepatosomatic index (IHS) was 4.1 ± 2.9.

Macroscopic characteristics: The GIT of the vizcaina comprises four macroscopically distinct regions: the oropharyngeal cavity, esophagus, stomach, and intestine (Fig. 1B, Fig. 1C). The esophagus is a short tubular segment,

Table 1
Morphological indices for the *C. mivartii* sample.

Organ		Mean ± SD	Maximum	Minimum
Weight (g)		117.5 ± 27.9	182.0	83.3
TL (cm)		23.2 ± 2.6	28.0	19.3
SL (cm)		18.1 ± 1.9	23.0	16.0
K		0.96 ± 0.24	1.58	0.44
HIS		4.07 ± 2.92	9.51	1.12
GSI	Male	0.8 ± 0.3	1.2	0.4
	Female	11.2 ± 4.7	16.0	1.1
Intestine (cm)		144.14 ± 38.49	242.0	102
IC		6.21 ± 1.44	8.8	4.42
RIL		7.92 ± 1.59	10.8	5.5
ZI		2.94 ± 0.63	4.3	2.12

Total length (TL), standard length (SL), condition factor (K), hepatosomatic index (HSI), gonadosomatic index (GSI), intestinal coefficient (IC), relative intestinal length (RIL), and Zihler index (ZI).

averaging 1.3 cm in length, with a moderately thick wall. The stomach, classified as curved or fundic (de Moraes et al., 1997), consists of three macroscopically and microscopically distinct regions: the cardiac, fundic, and pyloric. The cardiac region forms a tubular section posterior to the esophagus that expands into a short sac-like structure, the fundic region. The pyloric region is a long section with a thick wall and a prominent muscular tunic (muscular stomach). Pyloric caeca were observed posterior to the pyloric sphincter, connected to the anterior portion of the intestine.

The intestine of the *C. mivartii* is a long, densely coiled structure that fills the entire coelomic cavity. It is organized into paired spirals that fold upon themselves (Fig. 1) and have an average length of 144.14 ± 38.49 cm. The intestinal coefficient (IC) is 6.21 ± 1.44, the relative intestinal length (RIL) is 7.92 ± 1.59, and the Zihler's index is 2.94 ± 0.63 (Table 1). Macroscopically, the anterior segment of the intestine exhibits a slightly larger diameter than the middle and posterior segments.

Histology and histochemistry: Four concentric histological layers were identified throughout the GIT: The mucosa, in direct contact with the lumen of the organs, is subdivided into the epithelium and lamina propria. The lamina propria-submucosa, composed of a thick layer of loose connective tissue. The muscular layer consists of one or more layers of smooth and/or skeletal muscle. The serosa, the outermost layer of the GIT, is characterized by a thin layer of loose connective tissue that covers all regions of the GIT.

In the regions of the GIT analyzed in this study, no separation was observed between the lamina propria of the mucosal layer and the submucosal layer, which are usually separated by a thin muscular layer known as the *muscularis mucosae*. To emphasize this distinction, and as proposed by Sayyaf Dezfuli et al. (2018), the term lamina propria-submucosa will hereafter be used to refer to the thick layer of loose connective tissue situated between the epithelium and the muscular tunic. Based on the function of the organs, each layer may exhibit variations and specialized cellular structures, as summarized in Table 2 and described below.

Esophagus: In the esophagus, the mucosa displays longitudinal folds in the initial and final portions (Fig. 1C). The epithelium is pseudostratified columnar, with abundant goblet cells (mucus-producing cells) of oval morphology distributed throughout the length of the organ (Fig. 2A, Fig. 2F). Beneath the epithelium, mucous acinar glands composed of goblet

Table 2

Summary of histological and histochemical characteristics of the gastrointestinal tract of *C. mivartii* and potential associated physiological functions.

Region		Cell type	Staining intensity	Mucin type	Literature review	Associated function
Esophagus		Cylindrical and GC	Highest mucin production in the entire GIT	Predominantly acidic	Acidic mucins have higher viscosity, resistance to pathogen degradation (Verma et al., 2020). High microbial load in detritus (Zimmer, 2019); (Zimmer, 2024).	Ingestion and bioprotection
Glandular stomach		ColumnarAbsence of GC Oxynticopeptic	High intensity in the columnar apical end Mucus granules	Exclusively neutral	Neutral mucins are associated with protection from self-digestion, and contain cofactors (Anderson, 1986; Faccioli et al., 2014)	Peptidic digestion
Pyloric stomach		Columnar Absence of GC Koilin-like layer	High only in the koilin-like layer	Exclusively neutral	Koilin is a mucoprotein produced by epithelial cells and forms an abrasive membrane with greater development in high-fiber diets (Akester, 1986).	Protection against mechanical abrasion
Intestine	Anterior and middle	Enterocytes Sparse GC	Lowest mucin production in the entire GIT, low GC	Predominantly carboxylated acidic	Sialomucins present sialic acid residues in their structure, related to the interaction and selection of beneficial microorganisms (Gómez et al., 2013). Presence of high amounts of exogenous enzymes in the detritivore intestine (Farago, 2018).	Digestion and absorption Intestinal microbiome
	Posterior	Enterocytes and GC	Increased GC	Predominantly acidic Sulfomucins and carboxymucins	Ion absorption is associated with sulfated mucins: higher negative charge (Domeneghini, 1998). Enterocytes in this region present abundant microvilli (TEM).	Water and ion absorption. Lubrication

GC = Goblet cells.

cells were observed (Fig. 2A). Below the epithelial basement membrane, a thick layer of loose connective tissue, corresponding to the lamina propria-submucosa, was identified. Externally, the muscular layer consists of two layers of skeletal striated muscle. The inner layer is longitudinally arranged and is discontinuous in some regions. The outer muscle layer has a circular arrangement and is thicker. External to the muscular layer, a thin layer of loose connective tissue corresponding to the serosa or adventitia is observed (Fig. 2A).

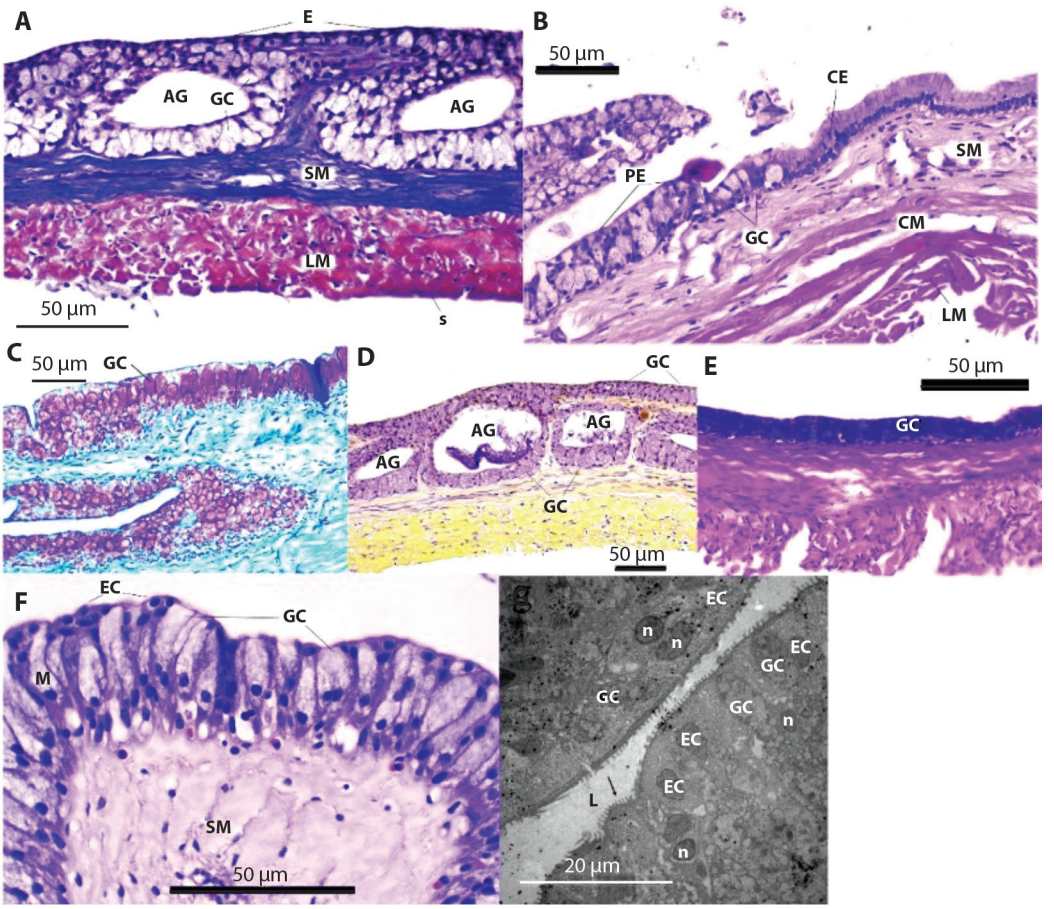

Fig. 2. Histological and histochemical characteristics of the esophagus of *C. mivartii*. **A.** Epithelium of the middle esophagus: ventrocaudal cephalic region between the pharynx and the stomach. Pseudostratified columnar epithelium (E), acinar glands (AG) formed by goblet cells (GC), lamina propria-submucosa (SM). Note the absence of muscularis mucosae. The muscular tunic is formed by skeletal striated muscle, the inner longitudinal layer (LM). Serous tunic (S) (Masson's Trichrome). **B.** Esophagus-stomach junction: anatomical boundary located at the entrance to the anterior abdominal cavity. Esophageal-gastric transition region, showing change from pseudostratified columnar epithelium (PE) with abundant goblet cells (GC) to simple columnar epithelium (CE) (H&E). **C.** Middle esophagus. The neutral mucins (fuchsia) in goblet cells (GC) (PAS). **D.** Acidic mucins (violet) in goblet cells (GC) and acinar glands (AG) (Mucicarmine). **E.** Predominance of acidic mucins (blue) in goblet cells (GC) (PAS/AB pH 2.5). **F.** Distal esophageal epithelium: the terminal segment of the esophagus before the stomach. Mucosal tunic (M) highlights the abundance of goblet cells (GC) among epithelial cells (EC) and submucosa (SM) in the distal esophageal epithelium before the gastric outlet (H&E). **G.** Ultrastructure of the luminal mucosa of the esophagus in the posterior cephalic region. Epithelial cells (EC) interspersed with goblet cells (GC) containing mucus vesicles of different electrodensity with oval nuclei (n). The arrow indicates microridges in the apical zone of epithelial cells that are in contact with the lumen (L).

Histochemical staining techniques revealed labeling for neutral mucins (Fig. 2C), sulfated acidic mucins, and carboxylated acidic mucins (Table 3). The staining of acidic mucins with mucicarmine exhibited moderate intensity (Fig. 2D) while AB staining showed strong intensity for carboxylated acidic mucins and moderate intensity for sulfated acidic mucins. In combined PAS/AB staining, acidic mucins predominate (strong intensity) (Fig. 2E), with the most intense labeling observed for carboxylated acidic mucins (Table 3). Additionally, labeling was exclusively found in goblet cells (Fig. 2E).

Stomach: The transition from the esophagus to the stomach is characterized by a change in the epithelium from a pseudostratified columnar to a simple columnar (Fig. 2B). The stomach is macroscopically divided into the cardial, fundic, and pyloric regions, each exhibiting specialized histological structures. These regions are differentiated into a glandular region (Fig. 3A, Fig. 3B, Fig. 3C, Fig. 3D, Fig. 3E) and a muscular region (Fig. 3F, Fig. 3G, Fig. 3H, Fig. 3I), which correspond to the cardiac and pyloric areas, respectively. The fundic region is a transitional zone between the glandular and muscular regions. The histological characteristics of each stomach region are described below.

Cardiac region: The cardial region of the stomach is composed of a broad mucosal layer that forms multiple short folds projecting into the lumen. The epithelium is simple columnar and contains numerous tubular gastric glands of oxynticopeptic cells (Fig. 3A). These oxynticopeptic cells have cuboidal morphology and eosinophilic granules when stained with H&E (Fig. 3B). The lamina propria-submucosa between the tubular glands is sparse, and beneath the mucosal layer, it appears as a thin layer of loose connective tissue. The muscular layer consists of two layers of smooth muscle: an inner circular layer and an outer longitudinal layer (Fig. 3A). Externally, a thin layer of loose connective tissue, corresponding to the serosa, is observed.

Fundic region: The fundic stomach is the middle region of the stomach and acts as a transitional zone where the mucosal layer becomes thinner due to the disappearance of the gastric glands found in the cardial region. The mucosa is lined with simple columnar epithelium and features some folds and gastric pits (Fig. 3D). Under the mucosa, there is a thin layer of loose connective tissue corresponding to the lamina propria-submucosa, which contains some blood vessels. The muscular layer consists of two smooth muscle layers: an inner circular layer and an outer longitudinal layer. Externally, a thin layer of loose connective tissue, corresponding to the serosa, is present.

Pyloric region: The pyloric stomach is the third segment of the stomach and is characterized by a thick, highly differentiated muscular wall (Fig. 3F). The mucosal layer is lined with simple columnar epithelium and features short folds (Fig. 3H, Fig. 3I). Over the epithelium, there is a thick keratinized layer, like the coiled layer observed in the ventriculus of birds (Fig. 3H, Fig. 3I). A thin layer of loose connective tissue corresponding to the lamina propria-submucosa is underneath the epithelium. The muscular layer in this region consists of a very thick layer of circular smooth muscle, making it the thickest muscular layer in this stomach segment (Fig. 3F, Fig. 3H). Externally, a thin layer of loose connective tissue corresponding to the serosa is observed.

The distribution of mucins in all regions of the stomach were exclusively neutral mucins (Table 3), with staining observed on the epithelial cells (Fig. 3D, Fig. 3E) and the coiled layer (Fig. 3G).

Intestine: Histologically, the intestine is divided into three segments: anterior, middle, and posterior. All segments feature a mucosal layer with digitiform folds projecting into the intestinal lumen, with shorter folds in the posterior segment (Fig. 4D, Fig. 4E, Fig. 4F, Fig. 4G). In the anterior and middle segments, some of the folds branch, creating the appearance of traversing the intestinal wall from side to side,

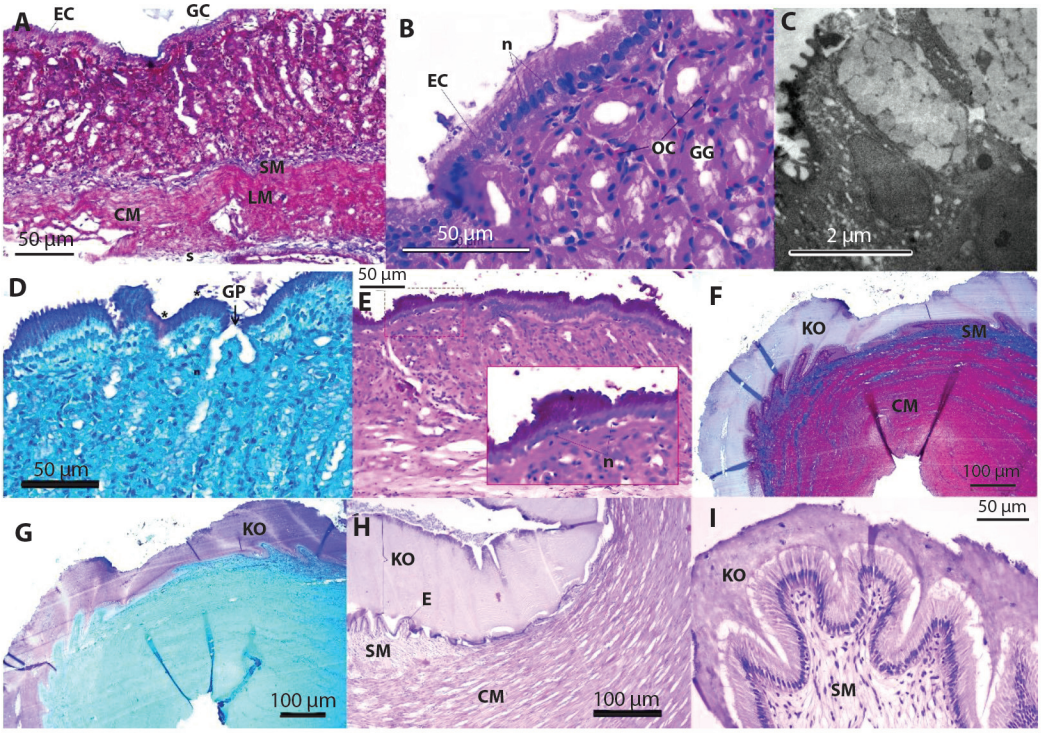

Fig. 3. Histological and histochemical characteristics of the stomach of *C. mivartii*. (GG) glandular stomach: anterior portion of the abdominal cavity immediately posterior to the esophagus, in the dorsal curvature of the U-shaped stomach. **A.** Histological layers: broad mucosa formed by tubular gastric glands (GG). Simple columnar epithelial cells (EC), lamina propria-submucosa (SM). Note the absence of muscularis mucosae. Smooth muscle tunic, inner circular layer (CM), and outer longitudinal layer (LM). Serous tunic (S) (Masson's Trichrome). **B.** Columnar epithelial cells (EC) with elongated morphology and oval nucleus in the basal third (n) are characteristic of enterocytes. Gastric glands (GG) are composed of oxynticopeptic cells (OC) with cuboidal morphology and eosinophilic granules (H&E). **C.** Ultrastructure of glandular stomach epithelium, showing vesicles with mucus granules released by exocytosis. Spaced microvilli in contact with the lumen are observed at the apical end of the cells. **D.** Neutral mucins in epithelial cells, staining on the apical region of cylindrical or columnar cells (*), oval nuclei (n) observed at the basal end of cells, and gastric pits (GP) (PAS). **E.** Exclusively neutral mucins in the apical end and in vesicles secreted by columnar cells (*) with and oval nuclei (n) (PAS/AB pH 2.5). **F.-I.** Muscular or pyloric stomach in the ventrocaudal abdominal region, posterior to the glandular stomach and anterior to the intestine. **F.** Histological layers: koilin-like layer (KO) over the epithelium, lamina propria-submucosa (SM) composed of connective tissue, and thick circular smooth muscle layer (CM) (Masson's Trichrome). **G.** Positive PAS staining in koilin-like layer (KO) (PAS). **H.** Detail of koilin-like layer (KO) over the epithelium (E), lamina propria-submucosa (SM) and circular smooth muscle tunic (CM) (H&E). **I.** Secondary folds of muscular stomach mucosa, submucosa (SM) and koilin-like layer (KO) (H&E).

forming a helix or spiral within the intestine (Fig. 4A). The mucosal layer in all segments is lined with simple columnar epithelium, predominantly consisting of columnar cells or enterocytes, particularly in the anterior segments (Fig. 4B). In the posterior segment, the number of columnar cells decreases while the number of goblet cells increases (Fig. 4F, Fig. 4G). Beneath the epithelium is a layer of loose connective tissue corresponding to the lamina propria-submucosa, followed by two layers of smooth muscle: the inner circular layer and the outer longitudinal layer, which form the muscular layer (Fig. 4B, Fig. 4G). Externally, a thin layer of loose connective tissue corresponding to the serosa is observed (Fig. 4B, Fig. 4G).

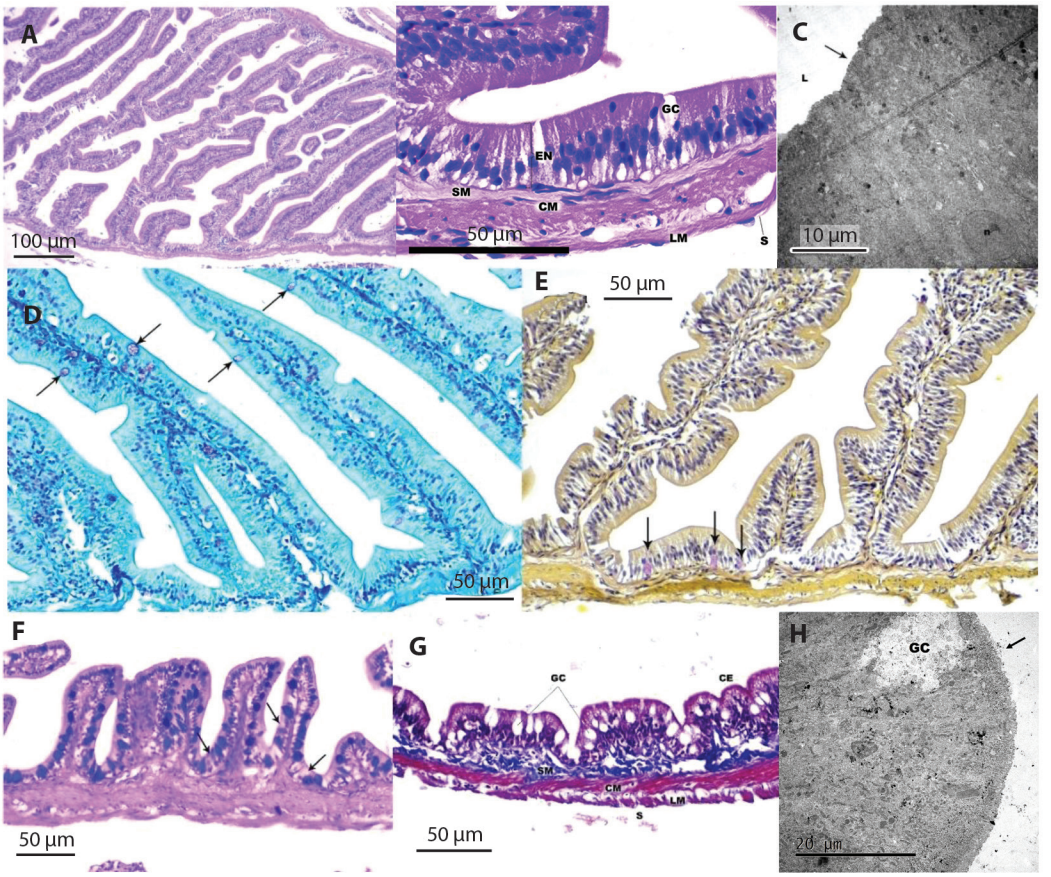

Fig. 4. Histological and histochemical characteristics of the intestine of *C. mivartii*. **A.** Helical folds in the anterior and middle intestine (H&E). **B.-D.** Anterior intestine: anterior abdominal region immediately posterior to the stomach. **B.** Simple columnar epithelium formed by cylindrical cells or enterocytes (EN) interspersed with sparse goblet cells (GC), supported by a connective tissue submucosa (SM), followed by two smooth muscle layers inner circular (CM) and outer longitudinal (LM) and a serous tunic (S) (H&E). **C.** Ultrastructure of anterior intestinal epithelium, showing elongated enterocytes with basal nucleus (n) and microvilli at the apical border (arrow) (L). **D.** Folds in the anterior intestine. Neutral mucin staining (fuchsia) in goblet cells (arrows). Note the sparse presence of goblet cells and longer folds compared to the posterior intestine (F and G). **E.** Middle intestine: central portion of the abdomen between the anterior and posterior intestines, folds showing positive staining for acidic mucins (violet), with sparse presence of goblet cells (arrows) (Mucicarmine). **F.-H.** Posterior intestine: distal segment of the digestive tract near the anus. **F.** Acidic and neutral mucin staining. Predominance of acidic mucins (blue). Arrows indicate goblet cells with combined staining for acidic (blue) and neutral (fuchsia) mucins. Note the increase in goblet cells and shorter folds (PAS/AB pH 2.5). **G.** Simple columnar epithelium (CE), lamina propria-submucosa (SM), inner circular (CM) and outer longitudinal (LM) smooth muscle layers, and serous tunic (S). The number of goblet cells (GC) is higher, and intestinal folds are shorter (Masson's Trichrome). **H.** Ultrastructure of posterior intestinal epithelium. Enterocytes with brush border apical surface (arrow), interspersed with goblet cells (GC) showing mucus granules of different electrodensity.

The histochemical analysis of the intestine showed the presence of all three types of mucins: Neutral, sulfated, acidic, and carboxylated (Table 3). Staining was observed exclusively in the goblet cells, which were scarce in the middle and anterior segments (Fig. 4D, Fig. 4E).

Mucicarmine staining exhibited a light intensity in the anterior and middle intestines (Fig. 4E) and a moderate intensity in

Table 3
Histochemical reactions in the mucosa of the gastrointestinal tract of *C. mivartii*.

Staining technique	Esophagus	Glandular stomach	Muscular stomach	Anterior intestine	Middle intestine	Posterior intestine
PAS	+++	+++	+++	+	+	++
AB pH 1.0	++	-	-	++	++	++
AB pH 2.5	+++	-	-	++	++	+++
PAS/AB pH 2.5	+++ Predominance of A	+++ N	+++ N	++ A + N	++ Predominance of A	++ Predominance of A
Mucicarmine	++	-	-	+	+	++
Cell type	CC	epithelial	Koilin layer	few CC	CC	CC

Staining intensity: (-) negative, (+) mild, (++) moderate, (+++) strong. Goblet cells (CC). Periodic acid-Schiff (PAS), Alcian Blue (AB). Neutral mucins (N), Acidic mucins (A).

the posterior intestine. Similarly, AB staining showed a moderate intensity in the anterior and middle intestines for both carboxylated and sulfated acidic mucins. In the posterior intestine, the AB staining intensity increased to the strong category for carboxylated mucins and moderate for sulfated mucins (Table 3).

The combined AB/PAS staining showed a slight predominance of acidic mucins in the few goblet cells of the anterior and middle segments. In the posterior segment, where goblet cells were more abundant, carboxylated acidic mucins predominated (Table 3, Fig. 4F).

Transmission Electron Microscopy (TEM): Transmission electron microscopy observations were conducted on the epithelium of different GIT regions to confirm the morphology of the epithelial cells. The presence of pseudostratified columnar epithelium interspersed with goblet cells containing mucus vesicles of varying electrodensity was observed in the esophagus. The epithelial cells exhibited microcrest at the apical surface (Fig. 2G). The glandular stomach displayed a simple columnar epithelium with mucus vesicles in the apical region and short, spaced microvilli on the luminal surface (Fig. 3C). In the intestine, the epithelial cells displayed the typical morphology of enterocytes, with brush border-like microvilli and oval nuclei located towards the basal domain (Fig. 4C). In the posterior intestine, mucus-producing cells were interspersed with enterocytes (Fig. 4H). The enterocytes of the posterior intestine exhibited abundant microvilli on the apical surface.

DISCUSSION

Biological indexes, such as the K and the IHS, are indicators of fish nutritional status and well-being. Values above one is considered acceptable, reflecting a healthy state and the absence of stress factors (Cifuentes et al., 2012; Cruz-Esquivel & Marrugo-Negrete, 2020; Ramírez & Pinilla, 2012). These indexes can vary due to seasonal fluctuations, reproductive periods, spawning, migration of the more robust individuals, food availability, and the fish's body shape (Cifuentes et al., 2012; Ramírez & Pinilla, 2012). According to the biological indexes reported in this study, the analyzed sample was in good condition: the IHS recorded values of 4.1 ± 2.9, indicating high metabolic activity and, consequently, high nutrient availability at the sampling site. The K value ranged from 0.96 ± 0.24, which is close to the value considered indicative of well-being. Since *C. mivartii* growth follows negative allometric scaling (Zuluaga-Gómez et al., 2014), meaning its length increases faster than its weight, K values below 1 are not necessarily related to its well-being, but rather to the species' specific morphology.

Regarding the sexual maturation indexes, the GSI showed significantly high values (11.2 ± 4.7 in females and 0.8 ± 0.3 in males), indicating an advanced stage of gonadal maturation. These values are consistent with the reproductive season during which the sample was collected from the Sogamoso River (March 2022). However, they do not correspond to the average size of the specimens captured for this study (23.2 ± 2.6 cm TL), which is below the reported size range for sexual maturation of the species (22.5 to 26.5 cm TL) (Mojica et al., 2012). The relationship between these morphological parameters (GSI and size) suggests that, for the sample in this study, sexual maturation occurs at smaller sizes than those reported in the literature for the species.

Anatomically, the digestive tract of *C. mivartii* consists of a short esophagus, a curved stomach with cardiac, fundic, and pyloric regions, pyloric caeca, and a very long, densely coiled intestine. This structure is similar to that reported in species of the Curimatidae family, such as *Steindachnerina notonota* (Da Silva, 2016), *Psectrogaster amazonica*, *Psectrogaster rutiloides*, *Potamorhina altamazonica*, and *Potamorhina latior* (Farago, 2018), as well as in species of the Prochilodontidae family, such as *Prochilodus lineatus* (de Moraes et al., 1997) and *Prochilodus scrofa* (Nachi et al., 1998), all of which feed on a detritus-based diet.

In macroscopic anatomy, the structure of the pyloric stomach, along with the length and folding of the intestine, is interpreted as an adaptation to detritus consumption. The pyloric stomach is responsible for mechanical digestion, enabling the grinding and sieving of organic matter that is difficult to digest, such as plant and fungal tissue (Bowen, 1983; Bowen, 2022; Moore et al., 2004). The length and curvature of the intestine, on the other hand, facilitate the retention of detritus for extended periods, maximizing nutrient absorption (Bowen, 1983). However, these structures are not exclusive to detritivores, as they have also been observed in herbivorous species like *Schizodon knerii* (Dos Santos et al., 2015) and omnivorous ones such as *Alestes baremoze* (Kasozi et al., 2017). Additionally, within detritivorous species of various orders, four distinct morphologies and mechanisms for digesting and assimilating detritus have been identified, one of which occurs in *Oreochromis niloticus* in the absence of a pyloric stomach (Bowen, 1981; Morrison & Wright, 1999). Therefore, the anatomical characteristics of the digestive tract are also influenced by phylogenetic factors, and the digestive specificities of a species may be reflected at the histological, histochemical, enzymatic, chemosensory, or even behavioral levels. This study focuses on the histological and histochemical characteristics of the digestive tract and their relation to the ability to assimilate a complex, low-nutrient substrate like detritus.

The esophagus of *C. mivartii* is a short tubular structure with longitudinal folds that increase the surface area of the epithelium and facilitate the directional movement of food toward the stomach (Fig. 1C). The esophageal epithelium is pseudo-stratified columnar, like *S. notonota* (Da Silva, 2016). Stratified and pseudo-stratified epithelia are common in the esophagus of fish due to their barrier functions, including stratified columnar (Londoño-Franco et al., 2017), stratified squamous (Dos Santos et al., 2015; Makino, 2010), and pseudo-stratified cuboidal (Alves et al., 2021) types. In particular, the pseudo-stratified epithelium is characterized by cellular proliferation and efficient molecular diffusion (Kia'i & Bajaj, 2019; Kurn & Daly, 2024; Norden, 2017). This proliferative capacity may be beneficial for the constant renewal of the esophageal epithelium, which is subjected to mechanical damage during ingestion.

In addition to its pseudostratified arrangement, the esophageal epithelium features cylindrical cells with short, widely spaced microcrests at their apical end (Fig. 2G). These structures have been documented in several studies on the ultrastructure of the fish esophagus. When analyzed using scanning electron microscopy (SEM), they are characterized as continuous elevations displaying a fingerprint-like microridges pattern (Arellano et al., 2001;

Carrassón et al., 2006; Faccioli, 2012; Mori, 2016). This microridges improves mucus adhesion to the epithelium, facilitating the flow of luminal contents and mitigating mechanical impact during ingestion (Wilson & Castro, 2010; Subramanian et al., 2022).

At the esophagus-stomach transition, the change from pseudostratified to simple columnar epithelium occurs abruptly (Fig. 2B). This contrasts with species such as *Semaprochilodus insignis* (Chaves & Vazzoler, 1984) and *A. baremoze* (Kasozi et al., 2017), where the columnar epithelium begins in the posterior esophagus and performs digestive or pre-digestive functions (Díaz et al., 2008). Conversely, in *C. mivartii*, the esophagus appears to be specialized for the secretion of large amounts of mucins. These mucins are produced by goblet cells distributed throughout the mucosa, as well as by mucous acinar glands, which are also composed of goblet cells.

According with Wilson & Castro (2010) noted that the presence of glands in the fish esophagus is rare. In most cases, these glands are in the esogaster and are associated with gastric glands, as observed in *A. baremoze* (Kasozi et al., 2017). However, in some species, such as *C. mivartii* (Fig. 2A), these acinar structures are composed of goblet cells and differ from gastric glands (Ferraris et al., 1987; Reifel & Travill, 1979; Wilson & Castro, 2010).

The production of abundant mucus in the esophagus is an important physiological trait in species suited for aquaculture, as it may aid in the consumption of dry feed. This trait has been previously reported in *Colossoma macropomum*, one of the most established species for captive breeding on a continental scale (Mori, 2016).

The muscular tunic of the *C. mivartii* esophagus consists of striated skeletal muscle under voluntary control, present in both the inner longitudinal and outer circular layers. This muscular configuration is unique to the esophagus in fish and contrasts with other gastrointestinal (GI) organs, where the inner layer is circular and the outer layer is longitudinal (Kapoor et al., 1975; Wilson & Castro, 2010). In species with taste buds in the esophagus, such as *Salminus brasiliensis* (Alves et al., 2021) and *S. knerii* (Dos Santos et al., 2015), striated muscle has been associated with food selection mechanisms, including the capacity for regurgitation (Alves et al., 2021). In *C. mivartii*, although taste buds were not observed in the esophagus, the presence of striated muscle may facilitate contractions for food transport to the stomach, distension to accommodate large food volumes, prevention of gastric content reflux (Diaz et al., 2006; Dos Santos et al., 2015), and potentially other non-chemosensory mechanisms involved in detritus selection.

Detritus selection represents an additional adaptation in detritivorous fish to improve nutrient extraction efficiency (Bowen, 1983). To further understand the nutritional strategies of *C. mivartii*, we recommend that future research explore the behavioral mechanisms underlying detritus selection (Ahlgren, 1996; Bowen, 1983; Lammons, 2009) and the chemosensory structures of the branchial arches (Da Silva, 2016).

The three regions of the *C. mivartii* stomach are composed of simple columnar epithelium and lack goblet cells. However, in the stomach, the columnar cells exhibit mucous-secreting activity (Wilson & Castro, 2010), fulfilling the function typically performed by goblet cells. Beneath the epithelium, the mucosa in the cardial and fundic regions contains tubular gastric glands, similar to those found in *A. baremoze* (Kasozi et al., 2017) and *P. lineatus* (Makino, 2010). These gastric glands consist of cuboidal cells with eosinophilic granules (Fig. 3B), called oxynticopeptic cells (Wilson & Castro, 2010). In fish, oxynticopeptic cells produce both hydrochloric acid and pepsinogen for acid digestion (Wilson & Castro, 2010). From now on, due to the abundance of gastric glands, the cardial and fundic regions will be collectively referred to as the glandular stomach.

In contrast to the glandular stomach, the mucosa of the pyloric stomach consists solely of columnar epithelium and lacks gastric glands or oxynticopeptic cells, like reports in *A. baremoze* (Kasozi et al., 2017) and in *P. lineatus*

(Makino, 2010). According to these authors, the enzymatic function of the glandular stomach and the mechanical function of the pyloric stomach are indicated by the presence and absence of gastric glands, respectively. Furthermore, it is suggested that in sediment-feeders and detritivorous species, the retention time of food in the glandular stomach is longer than in the pyloric stomach, facilitating slow chemical digestion and maximum interaction with digestive enzymes (Kasozi et al., 2017; Makino, 2010). In contrast, retention time in the pyloric stomach should be brief, as its function is mechanical digestion and gastric emptying into the intestine. Consistently, based on observations of the limited storage capacity of the stomachs in detritivorous fish of the Curimatidae family (Farago, 2018), it can also be inferred that the digestive process is not completed in the stomach and must continue in the intestine.

The muscular tunic of the entire stomach structure, including the cardial, fundic, and pyloric regions, is composed of smooth muscle, similar to what has been reported in other detritivorous species with a curved stomach, such as *Astyanax bimaculatus* (Cardoso, 2013), *S. knerii* (Dos Santos et al., 2015) and *S. notonota* (Da Silva, 2016). This contrasts with species like *P. lineatus*, where the striated skeletal muscle of the esophagus extends into the first third of the cardial stomach, allowing for the voluntary regurgitation of undesired food (Makino, 2010). The regurgitation capacity in *C. mivartii* appears to be limited, and the food selection mechanisms may be influenced by factors other than those previously suggested.

In the pyloric stomach, the smooth muscle tunic significantly increases in thickness, making the musculature the main characteristic of this stomach region, which is also referred to as the muscular stomach. Internally, the thickness of the muscular tunic forms longitudinal folds that narrow the lumen and facilitate friction during mechanical digestion (Fig. 3H). During the digestion process in the pyloric stomach, food is broken down into small particles to increase the surface area for contact with digestive enzymes and maximize nutrient extraction from detritus. While this grinding function may seem like compensation for the absence of teeth in *C. mivartii*, some authors suggest that it is an adaptation to microphagous feeding habits. This type of stomach allows the grinding of particles so small that teeth could not exert sufficient fracturing pressure (Arnette et al., 2024).

The function of the pyloric stomach has been studied in detritivorous species such as *P. lineatus*, where it was found that the sand and mineral particles ingested with detritus are crucial to the digestion process. In this species, minerals assist in grinding the food during the stomach's muscular contractions and form a sieve that prevents particles larger than 20 μm from passing into the intestine, retaining those that require more time for maceration. The same study demonstrated that the assimilation rate of amino acids increases sixfold with the ingestion and accumulation of particulate material in the pyloric stomach (Bowen, 2022). According to Bowen et al. (2006), the pyloric stomach is one of the most efficient mechanisms for detritus assimilation. The efficiency of organic matter assimilation, particularly amino acids, is directly related to the growth rate of fish. This characteristic is favorable for the adaptation of *C. mivartii* to fish farming systems. The species can utilize detritus from polyculture or feed with low nutritional value without requiring the addition of nutrients, and to reach the size and weight necessary for commercialization in a relatively short period of time, which translates into higher productive yield compared to species consuming organic matter with other intestinal mechanisms of detritus assimilation.

The differentiation between the glandular and muscular stomach occurs early in the embryonic development of *C. mivartii* and is crucial for nutrition from an exogenous food source. The glandular and muscular regions can be histologically identified at 15 days post-hatching (DPH) in larvae. By this time, the digestive system of fingerlings is sufficiently

developed to ingest food from the environment (Giraldo-Sarmiento, 2022).

In addition to the muscle layer, the mucosa of the pyloric stomach is covered by a thick, coiled layer (Fig. 1C), like the cuticle observed in the ventriculus of birds (Madkour et al., 2022; Madkour & Mohamed, 2019). This layer has been previously observed in species of the Curimatidae family, such as *S. notonota* (Da Silva, 2016; Da Silva et al., 2005). However, due to the intense PAS staining, it has been described as a mucus layer associated with lubrication and protection against mechanical damage. Nevertheless, the use of formalin in the methodology of this study dilutes the superficial mucus present in the tissues, leading us to exclude the possibility that it corresponds to a mucus layer.

Kapoor et al. (1975) summarized various descriptions of the inner pyloric stomach layer in Clupeidae, Channidae, certain Characidae, and Mugilidae as: a thick mucus layer, keratinized horny layer, non-cellular material layer, cuticle, or stratified epithelium with non-cellular/keratinized tissue containing isolated cell groups detached from the underlying epithelium. However, this structure has been studied in greater detail in the ventriculus of birds, where it is described as a koilin membrane secreted by the tubular glands of the ventriculus. This membrane acts as a grinding surface and is more developed in birds that consume high-fiber diets, such as insects and grains (Grujic-Injac et al., 1977; Wilkinson et al., 2018).

According to Akester (1986), it is a complex of proteins and polysaccharides, likely a mucoprotein, consistent with the strong PAS staining observed in this study. In fish, this membrane has been described as a koilin layer in the gizzard-like stomach of *Mugil cephalus*, where a higher density and more intense PAS staining were observed in fish fed commercial soybean-based diets compared to those fed yeast-based diets (Luzzana et al., 2005).

In the development of artificial diets for birds, it has been found that stimulating the function and development of the ventriculus by increasing the particle size ingested and adding structural components rich in insoluble fiber, such as shells, whole grains, and shavings, improves food utilization, nutrient assimilation rates, and ingestion frequency, resulting in higher productivity in captive breeding (Svihus, 2011). Similarly, this knowledge can be applied to the functioning of the pyloric stomach of *C. mivartii*, which operates through a mechanism like that of the gizzard in birds. To increase the efficiency of nutrient assimilation and the growth rate of the species, factors such as grain size in artificial feed, the incorporation of insoluble solids (sand and clay) into feed or crop bedding, and the provision of high fiber content through balanced feed or availability in crop bedding should be considered. An adaptation in the thickness of the koilin layer would also be expected depending on the composition of the feed and digestive efficiency. This approach is partially supported by the results of Bowen (2022), who demonstrates the indispensable role of mineral particles in the assimilation efficiency of the pyloric stomach. However, further studies are still needed to optimize the composition and size of the artificial diet.

Intestinal length is a morphological characteristic directly related to the difficulty of digesting ingested food. Consequently, detritivorous species typically exhibit high intestinal indexes (Duque-Correa et al., 2024). In *C. mivartii*, indexes such as the IC (6.21 ± 1.44) and RIL (7.92 ± 1.59) are considered by some authors to fall within the range of detritus-based diets, as they present values greater than three (Karachle & Stergiou, 2010). Similarly, in detritivorous species of the Curimatidae family, such as *P. altamazonica*, *P. latior*, *P. amazonica*, and *P. rutiloides*, indexes like the RIL range from 6-11 cm (Farago, 2018). The broad variation in intestinal indexes among detritivores can be associated with anatomical traits, such as the presence of intestinal folds and pyloric caeca, as well as the shape and size of the fish (Zavala-Camin, 1996). Additionally, the indexes may vary depending on the preference for specific substrates, such as the selection of animal or plant detritus (Karachle & Stergiou, 2010). In *P. latior*, for example, low

intestinal indexes are associated with a diet containing lower amounts of starch and lipids compared to other detritivorous species of the same genus. Moreover, significant deviations can occur within individuals of the same species due to detritus variability across different foraging areas (Farago, 2018).

Feeding behavior is another characteristic associated with intestinal length. When detritus is diluted with high proportions of inorganic matter, an increase in intestinal length enhances the interaction between digestive enzymes and the digestible resource (Duque-Correa et al., 2024). Ecological data for *C. mivartii* indicate that the species consumes detritus by suctioning submerged roots in shallow waters (Jiménez-Segura & Lasso, 2020). This behavior may reduce the ingestion of refractory material and promote the selection of higher-quality detritus, resulting in the expectation of lower intestinal indexes.

The diameter of the intestine is larger in the anterior region, as it is in contact with the stomach and pyloric caeca, where it receives food particles broken down through acidic and mechanical digestion. The anterior, middle, and posterior regions all exhibit intestinal folds; however, these folds are shorter in the posterior intestine to facilitate excretion, while they are more abundant and branched in the anterior and middle intestines to enhance nutrient absorption. The primary function of these folds is to increase the epithelial surface area and reduce the rate of food flow, thus improving the efficiency of nutrient absorption (De Seixas Filho et al., 2000). Between the anterior and middle intestines, there is a region where the folds branch and traverse the intestinal wall from side to side (Fig. 4A). This structure is like that observed in species such as *S. notonota* (Da Silva, 2016) and *P. scrofa* (Nachi et al., 1998), where it is associated with the spiral valve of elasmobranchs, a membranous organ that optimizes the length of the intestine (Wilson & Castro, 2010).

The intestinal epithelium consists of simple columnar cells, with an increasing abundance of goblet cells in the posterior region (Fig. 4F). The columnar cells exhibit the characteristic morphology of enterocytes: they are tall, slender, and have oval-shaped nuclei located toward the basal domain (Wilson & Castro, 2010). These same epithelial features were observed in the pyloric caeca of *C. mivartii*, suggesting that they may be associated with absorption functions, as discussed for *Prochilodus platensis* (Bowen, 1983) and *P. scrofa* (Nachi et al., 1998).

Muscularis mucosae was absent throughout the gastrointestinal tract of vizcaina, like *S. notonota* (Da Silva, 2016). Wilson and Castro (2010) state that teleosts lack *muscularis mucosae* layer; however, this layer has been reported in the stomach of *C. macropomum*, where it is associated with the emptying of gastric glands (Mori, 2016). In the cardiac stomach of *P. lineatus*, the absence of *muscularis mucosae* layer is compensated for by the three layers of smooth muscle in the muscular tunic, which support the mucosa (de Moraes et al., 1997). In vizcaína, the thickness of the muscular tunic in the glandular stomach is greater than in the esophagus and intestine, suggesting a potential supportive role in glandular activity.

In histochemical analyses, the staining intensity reflects the mucins produced by the cells or tissue (Neuhaus et al., 2007). In this study, the highest mucin production was observed in the esophagus (Table 3), produced by goblet cells and mucous acinar glands. The high mucus production in the esophagus compensates for the absence of salivary glands in fish, facilitating the lubrication of food passage to the stomach (Faccioli et al., 2014; Wilson & Castro, 2010). However, additional functions can be inferred based on the chemical structure of the mucins produced, as it will be discussed later. The role of mucus production in the esophagus for digestion is evident from studies on the species' embryonic development. In vizcaina larvae, exogenous feeding begins at 6 days post-embryo (DPE), at which point the esophagus develops, showing many goblet cells. Before this feeding phase, nutrients are provided by the yolk sac, without digestion needed. Therefore, the mouth is directly connected to the digestive tract, lined with simple columnar

epithelium and lacking goblet cells (Giraldo-Sarmiento, 2022).

In the esophagus of vizcaina, acidic and neutral mucins are produced homogeneously and with strong intensity throughout their entire length. This contrasts with findings in *Brycon amazonicus*, where the posterior region of the esophagus exclusively produces neutral mucins (Vidal et al., 2020). In vizcaina, acidic mucins predominate in the esophagus, with their negative charge enhancing mucus viscosity and resistance to pathogen degradation (Verma et al., 2020). This characteristic is associated with the high microbial load in freshly ingested detritus (Zimmer, 2019) (Table 2). Furthermore, the high adhesive and retention capacity of acidic mucins contributes to the solubilization of debris, facilitating chyme formation (Diaz et al., 2006), as observed in the mucus-mediated absorption mechanism of short-intestine herbivores such as *Arrhamphus sclerolepis krefftii* (Tibbetts, 1997).

In the stomach, mucin production was exclusively neutral, and unlike other regions of the GIT, staining was localized to the apical extremity of the columnar epithelial cells. The mucosecretory activity of columnar cells is well-documented; according to Wilson and Castro (2010), mucins are released into the lumen via exocytosis, as observed in certain images from this study (Fig. 3C, Fig. 3E). The primary function of neutral mucins in the stomach is to protect the mucosa from the corrosive effects of HCl and pepsin, which are produced by the oxynticopeptic cells in the glandular stomach. Additionally, these mucins provide cofactors for enzymatic activity (Anderson, 1986; Faccioli et al., 2014) and have been associated with the absorption of fatty acids and simple sugars (Bakke et al., 2010) (Table 2).

The gastric mucosa's protection relies on the mucus layer's thickness that coats the epithelium. To support this, columnar cells feature short microvilli on their apical surface (Fig. 3B), which aid in the distribution and maintenance of the superficial mucus layer (Arellano et al., 2001; Buddington & Christofferson, 1985; Moawad et al., 2017; Wilson & Castro, 2010). This mechanism ensures that the acidity of gastric juices does not reach the epithelium, preserving a pH gradient of approximately 2 units in the digestive lumen and nearly 7 units in the mucus layer adjacent to the mucosa (Allen, 1983).

The anterior and middle intestines exhibited the lowest mucus production within the GIT, a result of the sparse presence of goblet cells. In these regions, acidic mucins, predominantly carboxylated mucins (sialomucins), were the most abundant. These mucins are associated with interactions involving both pathogenic and commensal microorganisms (Gomez et al., 2013; McDonald et al., 2016; Yao et al., 2022). In fish infected with parasites, mucin glycosylation shifts towards sialylated and sulfated mucins. These alterations inhibit pathogen colonization and protect mucins from degradation by exogenous proteases. This mechanism preserves the integrity of the superficial mucus layer, preventing direct contact between pathogens and the host mucosa (Gomez et al., 2013; Neuhaus et al., 2007). In rainbow trout (*Oncorhynchus mykiss*), the highest levels of pathogen adhesion are observed in mucus layers rich in acidic mucins with sialylated and disialylated structures (Thomsson et al., 2022).

The effectiveness of the pathogen barrier depends on its adhesin to mucins and their subsequent removal from the superficial mucus layer. This layer is continuously renewed through the ongoing production of mucins by goblet cells, ensuring sustained protection (Werlang et al., 2019).

Sialomucins play a key role in stabilizing enzyme function (Díaz et al., 2008; Fiertak & Kilarski, 2002), act as recognition sites for microorganisms (Schauer, 2006), and are crucial for regulating the mutualistic relationships between commensal microorganisms in the intestinal microbiota. They provide a microenvironment conducive to adherence and serve as a nutrient source (Yao et al., 2022). Microorganisms capable of utilizing sialic acid as a carbon source can rapidly colonize the mucus layer and either establish themselves as commensals

or infect the tissue, depending on the host's immune response (McDonald et al., 2016).

The intestinal microbiome of fish plays a crucial role in supporting immune system function through competition with pathogens (Sehnal et al., 2021). It facilitates the metabolism of nutrients via exogenous enzymes not produced by the fish, such as β-glucanases, carbohydrases, cellulases, and chitinases, which are vital for the digestion of detritus (Merrifield & Rodiles, 2015). Farago (2018) assessed the activity of both endogenous and exogenous enzymes in four species of Curimatidae with detritivorous diets, observing high enzymatic activity in microbial extracts from the intestine (native or transient microbiota). The enzymes with the highest activity were alkaline phosphatase, N-acetyl-glucosamine, and β-glucanase, confirming that the direct or indirect action of microorganisms in the intestine aids in the assimilation of nutrients from detritus. Some researchers suggest that the intestinal length observed in herbivorous and detritivorous species maintains a symbiotic microbiome capable of breaking down recalcitrant food materials (Duque-Correa et al., 2024). The presence of commensal microorganisms in the intestines of fish has been a topic of interest in aquaculture for the development of probiotic diets (Gomez et al., 2013; Lazado & Caipang, 2014; Merrifield & Rodiles, 2015). Therefore, we propose studying the intestinal microbiome of *C. mivartii* in the intestine region where carboxylated mucins predominate.

A significant increase in goblet cells was observed in the posterior intestine, interspersed among the enterocytes (Fig. 4F, Fig 4H), exhibiting positive staining for neutral, sulfated, and carboxylated mucins. In terms of excretion functions, the lubrication of fecal flow is facilitated by the fluidity of neutral mucins and sialomucins, while sulfated mucins, being more viscous, help trap and retain molecules and pathogens (Domeneghini et al., 2005; Fiertak & Kilarski, 2002). The posterior intestine also absorbs ions, peptides, and water (Carrassón et al., 2006; Domeneghini et al., 2005; Faccioli et al., 2014; Verma et al., 2020). This capacity to absorb positively charged molecules is primarily associated with the polyanionic structure of sulfated mucins (Bakke et al., 2010; Domeneghini et al., 1998; Petrinec et al., 2005) and the presence of abundant microvilli on the enterocytes (Fig. 4H). The macroscopic and histochemical characteristics of the GIT of vizcaina demonstrate adaptations for detritus consumption and microphagy, with the pyloric stomach protected by a thick koilin-like layer responsive to fiber intake crucial consideration for captive breeding diets.

The comprehensive mapping of mucin distribution revealed neutral mucins throughout the GIT serving multiple functions, abundant sialomucins in the middle and anterior intestine facilitating microbial interactions and sulfated acidic mucins in the posterior intestine associated with ion and water retention. The remarkable mucus production in the esophagus, from both goblet cells and acinar glands, suggests potential benefits for dry food provision in captivity. This detailed characterization of *C. mivarti* GIT establishes a foundation for future research on pathologies, diet adaptability, and nutritional health status, potentially advancing captive breeding protocols for this native species, with future studies recommended to examine the oral apparatus due to its role in detritus selection mechanisms.

Ethical statement: The authors declare that they all agree with this publication and made significant contributions; that there is no conflict of interest of any kind; and that we followed all pertinent ethical and legal procedures and requirements. All financial sources are fully and clearly stated in the acknowledgments section. A signed document has been filed in the journal archives.

ACKNOWLEDGMENTS

The authors thank Piscícola San Silvestre S.A. and HISTOLAB for their technical contribution within the framework of the Management Program for protecting fish and fishing resources of the Sogamoso River and

its floodplain. This work was funded by ISAGEN S.A. (agreement 33/121 and 33/02168 ISAGEN-UdeA).

REFERENCES

Ahlgren, M. O. (1996). Selective ingestion of detritus by a north temperate omnivorous fish, the juvenile white sucker, Catostomus commersoni. *Environmental Biology of Fishes, 46*(4), 375–381. https://doi.org/10.1007/BF00005016

Akester, A. R. (1986). Structure of the glandular layer and koilin membrane in the gizzard of the adult domestic fowl (Gallus gallus domesticus). *Journal of Anatomy, 147*, 1–25.

Albus, U. (2012). Guide for the Care and Use of Laboratory Animals (8th edn). *Laboratory Animals, 46*(3), 267–268. https://doi.org/10.1258/la.2012.150312

Allen, A. (1983). Mucus: a protective secretion of complexity. *Trends in Biochemical Sciences, 8*(5), 169–173.

Alonso, F., Mirande, J. M., & Pandolfi, M. (2015). Gross anatomy and histology of the alimentary system of characidae (Teleostei: Ostariophysi: Characiformes) and potential phylogenetic information. *Neotropical Ichthyology, 13*(2), 273–286. https://doi.org/10.1590/1982-0224-20140137

Alves, A. P. C., Pereira, R. T., & Rosa, P. V. (2021). Morphology of the digestive system in carnivorous freshwater dourado *Salminus brasiliensis*. *Journal of Fish Biology, 99*(4), 1222–1235. https://doi.org/10.1111/jfb.14821

Anderson, T. A. (1986). Histological and cytological structure of the gastrointestinal tract of the luderick, *Girella tricuspidata* (Pisces, Kyphosidae), in relation to diet. *Journal of Morphology, 190*(1), 109–119. https://doi.org/10.1002/jmor.1051900110

Arellano, J. M., Storch, V., & Sarasquete, C. (2001). A histological and histochemical study of the oesophagus and oesogaster of the Senegal sole, *Solea senegalensis*. *European Journal of Histochemistry, 45*, 279–294. https://doi.org/10.4081/1638

Arnette, S. D., Simonitis, L. E., Egan, J. P., Cohen, K. E., & Kolmann, M. A. (2024). True grit? Comparative anatomy and evolution of gizzards in fishes. *Journal of Anatomy, 244*(2), 260–273. https://doi.org/10.1111/joa.13956

Autoridad Nacional de Acuicultura y Pesca. (2020). *Resolución 0955 de 2020*. https://www.aunap.gov.co

Bakke, A. M., Glover, C., & Krogdahl, Å. (2010). Feeding, digestion and absorption of nutrients. *Fish Physiology, 30*, 57–110. https://doi.org/10.1016/S1546-5098(10)03002-5

Bowen, S. H. (1981). Digestion and Assimilation of Periphytic Detrital Aggregate by Tilapia mossambica. *Transactions of the American Fisheries Society, 110*(2), 239–245. https://doi.org/10.1577/1548-8659(1981)110

Bowen, S. H. (1983). Detritivory in neotropical fish communities. *Environmental Biology of Fishes, 9*(2), 137–144. https://doi.org/10.1007/BF00690858

Bowen, S. H. (2022). Digestion and assimilation of benthic biofilm by Sábalo, *Prochilodus lineatus*. *Journal of Fish Biology, 100*(1), 107–116. https://doi.org/10.1111/jfb.14924

Bowen, S. H., Gu, B., & Huang, Z. (2006). Diet and Digestion in Chinese Mud Carp Cirrhinus molitorella Compared with Other *Ilyophagous Fishes*. *Transactions of the American Fisheries Society, 135*(5), 1383–1388. https://doi.org/10.1577/T05-158.1

Buddington, R. K., & Christofferson, J. P. (1985). Digestive and feeding characteristics of the chondrosteans. *Environmental Biology of Fishes, 14*(1), 31–41.

Burns, M. D. (2021). Adaptation to herbivory and detritivory drives the convergent evolution of large abdominal cavities in a diverse freshwater fish radiation (Otophysi: Characiformes). *Evolution, 75*(3), 688–705. https://doi.org/10.1111/evo.14178

Cardoso, N. das N. (2013). *Aspectos histológicos, histoquímicos e imuno-histoquímicos do tubo gastrintestinal de Astyanax bimaculatus (Linnaeus, 1758) nos reservatórios: do Funil, Santa Cecília e Ilha dos Pombos* [Dissertação de Mestrado]. Universidade Federal Rural do Rio de Janeiro, Seropédica, RJ, Brasil. https://tede.ufrrj.br/jspui/bitstream/jspui/3200/2/2013%20-%20Nathalia%20das%20Neves%20Cardoso.pdf

Carrassón, M., Grau, A., Dopazo, L. R., & Crespo, S. (2006). A histological, histochemical and ultrastructural study of the digestive tract of Dentex dentex (Pisces, Sparidae). *Histology and Histopathology, 21*(4–6), 579–593. https://doi.org/10.14670/HH-21.579

Chaves, C., & Vazzoler, G. (1984). Aspectos biológicos de peixes amazônicos. III – Anatomia microscópica do esôfago, estômago e cecos pilóricos de *Semaprochilodus insignis* (Characiforme: Prochilodontidae). *Acta Amazonica, 14*(3), 343–353.

Cifuentes, R., Gonzáles, J., Montoya, G., Jara, A., Ortíz, N., Piedra, P., & Habit, E. (2012). Relación longitud-peso y factor de condición de los peces nativos del río San Pedro (cuenca del río Valdivia, Chile). *Gayana Especial, 75*(2), 101–110.

Cruz-Esquivel, Á., & Marrugo-Negrete, J. (2020). Concentraciones de metilmercurio en *Prochilodus magdalenae* (teleostei : curimatidae) y *Hoplias malabaricus* (teleostei:erythrinidae) en la cuenca baja del río cauca-magdalena, norte de colombia. *Acta Biologica Colombiana, 27*(1), 28–35.

Da Silva, L. T. (2016). Adaptações morfológicas do trato digestório do peixe neotropical *Steindachnerina notonota* (Characiformes, Curimatidae) ao hábito alimentar detritívoro. Dissertação (Mestrado em Biologia Estrutural e Funcional) - Centro de Biociências, Universidade Federal do Rio Grande do Norte, Natal.

Da Silva, N., Gurgel, H., & Santana, M. (2005). Histologia do sistema digestório de sagüiru, *Steindachnerina notonota* (Miranda Ribeiro, 1937) (Pisces, Curimatidae), do Rio Ceará Mirim, Rio Grande do Norte, Brasil. *Boletim do Instituto de Pesca, 31*(1), 1–8.

de Moraes, M., Barbola, I. F., & Guedes, É. A. C. (1997). Alimentação e relações morfológicas com o aparelho digestivo do "curimbatá", *Prochilodus lineatus* (Valenciennes)(Osteichthyes, Prochilodontidae), de uma lagoa do sul do Brasil. *Revista Brasileira de Zoologia, 14*(1), 169–180.

de Seixas Filho, J. T., De Moura Brás, J., & De Mendonça Gomide, T. A. (2000). Anatomia funcional e morfometria dos intestinos e dos cecos pilóricos do teleostei (Pisces) de água doce Brycon orbignyanus (Valenciennes, 1849). *Revista Brasileira de Zootecnia, 29*(2), 313–324.

Diaz, A. O., Escalante, A. H., García, A. M., & Goldemberg, A. L. (2006). Histology and histochemistry of the pharyngeal cavity and oesophagus of the silverside *Odontesthes bonariensis* (Cuvier and Valenciennes). *Journal of Veterinary Medicine Series C: Anatomia, Histologia, Embryologia*, *35*(1), 42–46. https://doi.org/10.1111/j.1439-0264.2005.00654.x

Díaz, A. O., García, A. M., Devincenti, C. V., & Goldemberg, A. L. (2003). Morphological and histochemical characterization of the mucosa of the digestive tract in *Engraulis anchoita*. *Anatomia, Histologia, Embryologia*, *32*(6), 341–346. https://doi.org/10.1111/j.1439-0264.2003.00490.x

Díaz, A. O., García, A. M., & Goldemberg, A. L. (2008). Glycoconjugates in the mucosa of the digestive tract of *Cynoscion guatucupa*: A histochemical study. *Acta Histochemica*, *110*(1), 76–85. https://doi.org/10.1016/j.acthis.2007.08.002

Domeneghini, C., Arrighi, S., Radaelli, G., Bosi, G., & Veggetti, A. (2005). Histochemical analysis of glycoconjugate secretion in the alimentary canal of *Anguilla anguilla* L. *Acta Histochemica*, *106*(6), 477–487. https://doi.org/10.1016/j.acthis.2004.07.007

Domeneghini, C., Straini, R. P., & Veggetti, A. (1998). Gut glycoconjugates in *Sparus aurata* L. (Pisces, Teleostei). A comparative histochemical study in larval and adult ages. *Histology and Histopathology*, *13*(2), 359–372. https://doi.org/10.14670/HH-13.359

Dos Santos, M. L., Arantes, F. P., Santiago, K. B., & Dos Santos, J. E. (2015). Morphological characteristics of the digestive tract of *Schizodon knerii* (Steindachner, 1875) (Characiformes: Anostomidae): An anatomical, histological and histochemical study. *Anais da Academia Brasileira de Ciências*, *87*(2), 867–878. https://doi.org/10.1590/0001-3765201520140230

Duque-Correa, M. J., Clements, K. D., Meloro, C., Ronco, F., Boila, A., Indermaur, A., Salzburger, W., & Clauss, M. (2024). Diet and habitat as determinants of intestine length in fishes. *Reviews in Fish Biology and Fisheries*, *34*(3), 1017–1034. https://doi.org/10.1007/s11160-024-09853-3

Faccioli, C. K. (2012). *Estudos morfológicos e histoquímicos do tubo digestivo de Hemisorubim platyrhynchos* [Tesis de maestría]. Universidade Estadual Paulista.

Faccioli, C. K., Chedid, R. A., Amaral, A. Ô. C. do, Franceschini Vicentini, I. B., & Vicentini, C. A. (2014). Morphology and histochemistry of the digestive tract in carnivorous freshwater *Hemisorubim platyrhynchos* (Siluriformes: Pimelodidae). *Micron*, *64*, 10–19. https://doi.org/10.1016/j.micron.2014.03.011

Farago, T. L. B. (2018). *Utilização do detrito por espécies de peixes amazônicas: assimilação diferencial e partilha de recurso* [Tese de doutorado]. Instituto Nacional de Pesquisas da Amazônia.

Ferraris, R. P., Tan, J. D., & De La Cruz, M. C. (1987). Development of the digestive tract of milkfish, *Chanos chanos* (Forsskål): Histology and histochemistry. *Aquaculture*, *61*(3–4), 241–257. https://doi.org/10.1016/0044-8486(87)90153-0

Fiertak, A., & Kilarski, W. M. (2002). Glycoconjugates of the intestinal goblet cells of four cyprinids. *Cellular and Molecular Life Sciences*, *59*, 1724–1733. https://doi.org/10.1007/PL00012490

Fletcher, T. C., Jones, R., & Reid, L. (1976). Identification of glycoproteins in goblet cells of epidermis and gill of plaice (*Pleuronectes platessa* L.), flounder (*Platichthys flesus* L.) and rainbow trout (*Salmo gairdneri* Richardson). *Histochemical Journal*, *8*, 597–608.

Giraldo-Sarmiento, R. (2022). *Desarrollo ontogénico y morfofuncional de alevinos de Prochilodus magdalenae y Curimata mivartii con fines de conservación y seguridad alimentaria* [Tesis doctoral]. Universidad de Córdoba.

Gomez, D., Sunyer, J. O., & Salinas, I. (2013). The mucosal immune system of fish: The evolution of tolerating commensals while fighting pathogens. *Fish & Shellfish Immunology*, *35*(6), 1729–1739. https://doi.org/10.1016/j.fsi.2013.09.032

Gona, O. (1979). Mucous glycoproteins of teleostean fish: A comparative histochemical study. *Histochemical Journal*, *11*, 709–718.

Grujic-Injac, B., Dimitrijevic, M., Lajsic, S., Stefanovic, D., & Micovic, I. (1977). The structure of a new phospholipid from the koilin-glandular layer of chicken

gizzard. *Hoppe-Seyler's Zeitschrift für Physiologische Chemie*, *358*, 499–504.

Guisande, C., Pelayo-Villamil, P., Vera, M., Manjarrés-Hernández, A., Carvalho, M. R., Vari, R. P., Jiménez, L. F., Fernández, C., Martínez, P., Prieto-Piraquive, E., Granado-Lorencio, C., & Duque, S. R. (2012). Ecological factors and diversification among Neotropical characiforms. *International Journal of Ecology*, *2012*, 610419. https://doi.org/10.1155/2012/610419

Hincapié-Cruz, J. P., & Márquez, E. J. (2021). Phenotypic variation of the fishes *Curimata mivartii* (Characiformes: Curimatidae) and *Pimelodus grosskopfii* (Siluriformes: Pimelodidae) in lotic and lentic habitats. *Revista de Biología Tropical*, *69*(2), 434–444. https://doi.org/10.15517/rbt.v69i2.41708

Jiménez-Segura, L. (2016). *Curimata mivartii*, Vizcaína. *The IUCN Red List of Threatened Species*. https://doi.org/10.2305/IUCN.UK.2016-1.RLTS.T167634A61472671.en

Jiménez-Segura, L., & Lasso, C. A. (2020). XIX. Peces de la cuenca del río Magdalena, Colombia: Diversidad, conservación y uso sostenible. *Serie Editorial Recursos Hidrobiológicos y Pesqueros Continentales de Colombia*.

Jiménez-Segura, L. F., Palacio, J., & Leite, R. (2010). River flooding and reproduction of migratory fish species in the Magdalena River basin, Colombia. *Ecology of Freshwater Fish*, *19*(2), 178–186. https://doi.org/10.1111/j.1600-0633.2009.00402.x

Kapoor, B. G., Smit, H., & Verighina, I. A. (1975). The alimentary canal and digestion in teleosts. *Advances in Marine Biology*, *13*, 109–239.

Karachle, P. K., & Stergiou, K. I. (2010). Intestine morphometrics of fishes: A compilation and analysis of bibliographic data. *Acta Ichthyologica et Piscatoria*, *40*(1), 45–54. https://doi.org/10.3750/AIP2010.40.1.06

Kasozi, N., Degu, G. I., Mukalazi, J., Kato, C. D., Kisekka, M., Owori Wadunde, A., Kityo, G., & Namulawa, V. T. (2017). Histomorphological description of the digestive system of pebbly fish, *Alestes baremoze* (Joannis, 1835). *The Scientific World Journal*, *2017*, 8591249. https://doi.org/10.1155/2017/8591249

Kia'i, N., & Bajaj, T. (2019). Histology, respiratory epithelium. *StatPearls*.

Kurn, H., & Daly, D. T. (2024). Histology, epithelial cell. *StatPearls*.

Lammons, M. L. (2009). *Mud and mucus: Feeding selectivity in a suspension-feeding detritivorous fish* [Master's thesis]. The College of William and Mary. https://dx.doi.org/doi:10.21220/s2-gbgr-2f33

Landínez-García, R. M., & Márquez, E. J. (2018). Microsatellite loci development and population genetics in Neotropical fish *Curimata mivartii* (Characiformes: Curimatidae). *PeerJ*, *6*, e5959. https://doi.org/10.7717/peerj.5959

Lasso, C. A., Córdoba, E. A., Jiménez-Segura, L. F., Ramírez-Gil, H., Morales-Betancourt, M., Ajiaco-Martínez, R. E., Gutiérrez, F. de P., Oviedo, J. S. U., Torres, S. E. M., & Ochoa, A. I. S. (2011). I. Catálogo de los recursos pesqueros continentales de Colombia. *Serie Editorial Recursos Hidrobiológicos y Pesqueros Continentales de Colombia*. Instituto de Investigación de Recursos Biológicos Alexander von Humboldt.

Lavoué, S., Arnegard, M. E., Rabosky, D. L., McIntyre, P. B., Arcila, D., Vari, R. P., & Nishida, M. (2017). Trophic evolution in African citharinoid fishes (Teleostei: Characiformes) and the origin of intraordinal pterygophagy. *Molecular Phylogenetics and Evolution*, *113*, 23–32. https://doi.org/10.1016/j.ympev.2017.05.001

Lazado, C. C., & Caipang, C. M. A. (2014). Mucosal immunity and probiotics in fish. *Fish & Shellfish Immunology*, *39*(1), 78–89. https://doi.org/10.1016/j.fsi.2014.04.015

Londoño-Franco, L. F., Laverde-Trujillo, L. M., & Muñoz-García, F. G. (2017). Descripción anatómica e histológica del aparato digestivo de la sabaleta (*Brycon henni*), Antioquia, Colombia. *Revista de Investigaciones Veterinarias del Perú*, *28*(3), 490–504. https://doi.org/10.15381/rivep.v28i3.13354

Luzzana, U., Valfre, F., Mangiarotti, M., Domeneghini, C., Radaelli, G., Moretti, V. M., & Scolari, M. (2005). Evaluation of different protein sources in fingerling grey mullet *Mugil cephalus* practical diets. *Aquaculture International*, *13*, 291–303. https://doi.org/10.1007/s10499-004-3099-9

López-Casas, S., Jiménez-Segura, L. F., Agostinho, A. A., & Pérez, C. M. (2016). Potamodromous migrations in the Magdalena River basin: Bimodal reproductive patterns in neotropical rivers. *Journal of Fish Biology, 89*(1), 1–135. https://doi.org/10.1111/jfb.12941

Madkour, F. A., & Mohamed, A. A. (2019). Macro-microscopical anatomy of the gizzard of Egyptian laughing dove and rock pigeon. *Assiut Veterinary Medical Journal*, *65*(161), 278–285. https://doi.org/10.21608/AVMJ.2019.168916

Madkour, F. A., Mohamed, S. A., Abdalla, K. E. H., & Ahmed, Y. A. (2022). Post-hatching development of ventriculus in Muscovy duck: Light and electron microscopic study. *Journal of Advanced Veterinary Research*, *12*(1), 42–53.

Makino, L. C. (2010). *Estrutura, ultraestrutura e histoquímica do aparelho digestório do Prochilodus lineatus. Análise da diversidade da microbiota intestinal de Prochilodus lineatus e Pterygoplichthys anisitsi* [Tesis doctoral]. Universidade Estadual Paulista.

Mantle, M., & Allen, A. (1981). Characterization of small-intestinal mucus glycoproteins. *Biochemical Journal*, *195*, 267–275.

McDonald, N. D., Lubin, J., Chowdhury, N., & Boyd, E. F. (2016). Host-derived sialic acids are an important nutrient source required for optimal bacterial fitness in vivo. *mBio*, *7*(2), e02237-15. https://doi.org/10.1128/mBio.02237-15

Merrifield, D. L., & Rodiles, A. (2015). The fish microbiome and its interactions with mucosal tissues. En *Mucosal Health in Aquaculture*. Elsevier. https://doi.org/10.1016/B978-0-12-417186-2/00010-8

Moawad, U., Awaad, A., & Tawfiek, M. (2017). Histomorphological, histochemical, and ultrastructural studies on the stomach of the adult African catfish (*Clarias gariepinus*). *Journal of Microscopy and Ultrastructure*, *5*(3), 155–166. https://doi.org/10.1016/j.jmau.2016.08.002

Mojica, J. I., Usma, J. S., Álvarez-León, R., & Lasso, C. A. (Eds.). (2012). *Libro rojo de peces dulceacuícolas de Colombia*. Instituto de Investigación de Recursos Biológicos Alexander von Humboldt.

Montes-Petro, C., Atencio-García, V., Estrada-Posada, A., & Yepes-Blandón, J. (2019). Reproducción en cautiverio de vizcaína *Curimata mivartii* con extracto pituitario de carpa. *Orinoquia*, *23*(2), 63–70.

Moore, J. C., Berlow, E. L., Coleman, D. C., de Ruiter, P. C., Dong, Q., Hastings, A., Johnson, N. C., McCann, K. S., Melville, K., Morin, P. J., Nadelhoffer, K., Rosemond, A. D., Post, D. M., Sabo, J. L., Scow, K. M., Vanni, M. J., & Wall, D. H. (2004). Detritus, dinámica trófica y biodiversidad. *Ecology Letters, 7*, 584–600. *https://doi.org/10.1111/j.1461-0248.2004.00606.x*

Mori, R. H. (2016). *Análises morfológicas, histoquímicas e ultraestruturais do tubo digestivo de tambaqui Colossoma macropomum (Cuvier, 1816)* [Tese de doutorado, Universidade Estadual Paulista]. Universidade Estadual Paulista.

Morrison, C. M., & Wright, J. R., Jr. (1999). A study of the histology of the digestive tract of the Nile tilapia. *Journal of Fish Biology, 54*, 597–606.

Nachi, A. M., Hernandez-Blazquez, F. J., Barbieri, R. L., Leite, R. G., Ferri, S., & Phan, M. T. (1998). Intestinal histology of a detritivorous (iliophagous) fish *Prochilodus scrofa* (Characiformes, Prochilodontidae). *Annales des Sciences Naturelles - Zoologie et Biologie Animale, 19*(2), 81–88. https://doi.org/10.1016/S0003-4339(98)80002-6

Neuhaus, H., van der Marel, M., Caspari, N., Meyer, W., Enss, M. L., & Steinhagen, D. (2007). Biochemical and histochemical study on the intestinal mucosa of the common carp *Cyprinus carpio* L., with special consideration of mucin glycoproteins. *Journal of Fish Biology, 70*(5), 1523–1534. https://doi.org/10.1111/j.1095-8649.2007.01438.x

Norden, C. (2017). Pseudostratified epithelia—Cell biology, diversity and roles in organ formation at a glance. *Journal of Cell Science, 130*(11), 1859–1863. https://doi.org/10.1242/jcs.192997

Petrinec, Z., Nejedli, S., Kužir, S., & Opačak, A. (2005). Mucosubstances of the digestive tract mucosa in northern pike (*Esox lucius* L.) and European catfish (*Silurus glanis* L.). *Veterinarski Arhiv, 75*(4), 317–327.

Ramírez, A., & Pinilla, G. (2012). Hábitos alimentarios, morfometría y estados gonadales de cinco especies de peces en diferentes periodos climáticos en el río Sogamoso (Santander, Colombia). *Acta Biológica Colombiana, 17*(2), 241–258.

Reifel, C. W., & Travill, A. A. (1979). Structure and carbohydrate histochemistry of the intestine in ten teleostean species. *Journal of Morphology, 162*(3), 343–359. https://doi.org/10.1002/jmor.1051620305

Salinas, I., & Parra, D. (2015). Fish mucosal immunity: Intestine. En B. H. Beck, & E. Peatman (Eds.), *Mucosal health in aquaculture* (pp. 135–170). Academic Press. https://doi.org/10.1016/B978-0-12-417186-2.00006-6

Sayyaf Dezfuli, B., Manera, M., Bosi, G., Merella, P., Depasquale, J. A., & Giari, L. (2018). Intestinal granular cells of a cartilaginous fish, thornback ray *Raja clavata*: Morphological characterization and expression of different molecules. *Fish & Shellfish Immunology, 75*, 172–180. https://doi.org/10.1016/j.fsi.2018.02.019

Schauer, R. (2006). Sialic acids: Fascinating sugars in higher animals and man. *Zoology, 107*(1), 49–64. https://doi.org/10.1016/j.zool.2003.10.002

Sehnal, L., Brammer-Robbins, E., Wormington, A. M., Blaha, L., Bisesi, J., Larkin, I., Martyniuk, C. J., Simonin, M., & Adamovsky, O. (2021). Microbiome composition and function in aquatic vertebrates: Small organisms making big impacts on aquatic animal health. *Frontiers in Microbiology, 12*, 567408. https://doi.org/10.3389/fmicb.2021.567408

Steindachner, F. (1878). Zur Fisch-Fauna des Magdalenen-Stromes. *Denkschriften der Kaiserlichen Akademie der Wissenschaften in Wien, Mathematisch-Naturwissenschaftliche Classe, 39*, 19–78.

Svihus, B. (2011). The gizzard: Function, influence of diet structure and effects on nutrient availability. *World's Poultry Science Journal, 67*(2), 207–223. https://doi.org/10.1017/S0043933911000249

Sánchez-Duarte, P., & Lasso, C. A. (2013). Evaluación del impacto de las medidas de conservación del Libro Rojo de peces dulceacuícolas (2002–2012) en Colombia. *Biota Colombiana, 14*(2), 17–32.

Subramanian, D. A., Langer, R., & Traverso, G. (2022). Mucus interaction to improve gastrointestinal retention and pharmacokinetics of orally administered nano-drug delivery systems. *Journal of Nanobiotechnology*, *20*(1), 362. https://doi.org/10.1186/s12951-022-01539-x

Thomsson, K. A., Benktander, J., Quintana-Hayashi, M. P., Sharba, S., & Lind, K. (2022). Mucin O-glycosylation and pathogen binding ability differ between rainbow trout epithelial sites. *Fish & Shellfish Immunology, 131*, 349–357. https://doi.org/10.1016/j.fsi.2022.10.012

Tibbetts, I. R. (1997). The distribution and function of mucous cells and their secretions in the alimentary tract of *Arrhamphus sclerolepis krefftii*. *Journal of Fish Biology, 50*(4), 809–820. https://doi.org/10.1006/jfbi.1996.0347

Vari, R. P. (1989a). A phylogenetic study of the neotropical characiform family Curimatidae (Pisces: Ostariophysi). *Smithsonian Contributions to Zoology, 471*, 1–71.

Vari, R. P. (1989b). Systematics of the neotropical characiform genus *Curimata* Bosc (Pisces: Characiformes). *Smithsonian Contributions to Zoology, 474*, 1–63.

Verma, C. R., Gorule, P. A., Kumkar, P., Kharat, S. S., & Gosavi, S. M. (2020). Morpho-histochemical adaptations of the digestive tract in Gangetic mud-eel *Ophichthys cuchia* (Hamilton, 1822) support utilization of mud-dwelling prey. *Acta Histochemica, 122*(7), 151602. https://doi.org/10.1016/j.acthis.2020.151602

Vidal, M. R., Gardinal, M. V. B., Vicentini, I. B. F., Santos, D. D., de Jesus, F. L., & Vicentini, C. A. (2020). Morphological and histochemical characterisation of the mucosa of the digestive tract in matrinxã *Brycon amazonicus* (Teleostei: Characiformes). *Journal of Fish Biology, 96*(2), 251–260. https://doi.org/10.1111/jfb.14217

Werlang, C., Cárcarmo-Oyarce, G., & Ribbeck, K. (2019). Engineering mucus to study and influence the microbiome. *Nature Reviews Materials, 4*(2), 134–145. https://doi.org/10.1038/s41578-018-0079-7

Wilkinson, N., Dinev, I., Aspden, W. J., Hughes, R. J., Christiansen, I., Chapman, J., Gangadoo, S., Moore, R. J., & Stanley, D. (2018). Ultrastructure of the gastrointestinal tract of healthy Japanese quail (*Coturnix japonica*) using light and scanning electron microscopy. *Animal Nutrition, 4*(4), 378–387. https://doi.org/10.1016/j.aninu.2018.06.006

Wilson, J. M., & Castro, L. F. C. (2010). Morphological diversity of the gastrointestinal tract in fishes. En M. Grosell, A. P. Farrell, & C. J. Brauner (Eds.), *Fish physiology* (Vol. 30, pp. 1–55). Academic Press. https://doi.org/10.1016/S1546-5098(10)03001-3

Yao, Y., Kim, G., Shafer, S., Chen, Z., Kubo, S., Ji, Y., Luo, J., Yang, W., Perner, S. P., Kanellopoulou, C., Park, A. Y., Jiang, P., Li, J., Baris, S., Aydiner, E. K., Ertem, D., Mulder, D. J., Warner, N., Griffiths, A. M., … Lenardo, M. J. (2022). Mucus sialylation determines intestinal host-commensal homeostasis. *Cell, 185*(7), 1172–1188.e28. https://doi.org/10.1016/j.cell.2022.02.013

Zavala-Camin, L. A. (1996). Introdução aos estudos sobre alimentação natural em peixes. EDUEM.

Zimmer, M. (2019). Detritus. En B. Fath (Ed.), *Encyclopedia of ecology* (2nd ed., Vol. 3, pp. 292–301). Elsevier. https://doi.org/10.1016/B978-0-12-409548-9.10918-2

Zimmer, M. (2024). *Detritus: Reference Module in Earth Systems and Environmental Sciences*. Elsevier. https://doi.org/10.1016/B978-0-443-21964-1.00016-1

Zuluaga-Gómez, A., Giarrizzo, T., Andrade, M., & Arango-Rojas, A. (2014). Length-weight relationships of 33 selected fish species from the Cauca River Basin, trans-Andean region, Colombia. *Journal of Applied Ichthyology, 30*(5), 1077–1080. https://doi.org/10.1111/jai.12435